

Asymptotic Floquet states of a periodically driven spin-boson system in the nonperturbative coupling regime

Luca Magazzù,¹ Sergey Denisov,^{1,2,3} and Peter Hänggi^{1,4}

¹*Institute of Physics, University of Augsburg,*

Universitätsstrasse 1, D-86135 Augsburg, Germany

²*Department of Applied Mathematics, Lobachevsky State*

University of Nizhny Novgorod, Nizhny Novgorod 603950, Russia

³*Sumy State University, Rimsky-Korsakov Street 2, 40007 Sumy, Ukraine*

⁴*Nanosystems Initiative Munich, Schellingstraße 4, D-80799 München, Germany*

(Dated: March 9, 2024)

As a paradigmatic model of open quantum system, the spin-boson model is widely used in theoretical and experimental investigations. Beyond the weak coupling limit, the spin dynamics can be described by a time-nonlocal generalized master equation with a memory kernel accounting for the dissipative effects induced by the bosonic environment. When the spin is additionally modulated by an external time-periodic electromagnetic field, the interplay between dissipation and modulations yields a spectrum of nontrivial asymptotic states, especially in the regime of nonlinear response. Here we implement a method for the evaluation of Floquet dynamics in non-Markovian systems [L. Magazzù *et al.*, Phys. Rev. A **96**, 042103 (2017)] to find these strongly non-equilibrium states.

I. INTRODUCTION

The spin-boson model [1] has been – and still remains – the subject of extensive studies, as it constitutes an archetype of open quantum system [2–7]. This model describes a single spin (qubit) coupled to a dissipative environment consisting of an infinite number of bosonic modes. The spin-boson model is of relevance in a great variety of fields of physics and chemistry, with applications in electron tunneling [2, 3], excitation transport in biological complexes [4, 5], and superconducting qubit technologies [6, 7], to name but a few.

In the regime of weak coupling to the bosonic environment, the dynamics of the spin can be described by a master equation derived within the Born-Markov approximation [8] and improvements over this approximation, see for example Refs. [9, 10]. Different techniques have been developed to deal with the more challenging coupling regimes which are beyond the perturbative limit. The current toolbox includes stochastic Schrödinger [11] and Liouville [12] equations, different variational approaches [13–16], numerical renormalization group methods [17], sparse polynomial

approach [18], reaction coordinate [19–21] and combined thermofield/chain [22] mappings.

Within the path integral approach, the influence of the environment on the evolution an open system (described with a reduced density matrix) is captured by the Feynman-Vernon influence functional [23]. This formulation is suitable for numerically exact treatments such as Quantum Monte Carlo [24–26], the quasi-adiabatic propagator path-integral method [4, 27, 28], and hierarchical equations of motion (HEOM) [29–32], but also provides an analytical tool that can deal with the opposite limits of weak [33] and strong coupling [1], and even provides approximation schemes that bridge this two regimes [34, 35].

Different coupling regimes, corresponding different spin dynamics (coherent and incoherent), have been attained with superconducting qubits [6, 7, 36, 37], currently one of the most popular platforms for quantum computing and quantum simulations [38–41]. In particular, a setup based on a flux qubit coupled to a transmission line has been proposed to cover coupling strengths ranging from weak to ultra-strong [37]. The same setup has been recently used to investigate the impact of a monochromatic driving on the qubit dynamics in different dissipation and driving regimes [42]. Experimental results have been appropriately accounted for by the path integral approach within an approximation scheme which is nonperturbative with respect to the coupling strength. In this approach, the driven spin-boson dynamics is described with a generalized master equation (GME) for the spin, where a memory kernel constructed on a microscopical basis accounts for both the driving and dissipation [43].

While this GME for the spin dynamics cannot be evaluated within the standard Floquet formalism (because of the time-nonlocal character of the dynamics), the evolution of the spin-boson system in the full Hilbert space is governed by a time-periodic Hamiltonian and, therefore, can be – though only formally – handled with the standard Floquet theory. The Floquet theory also applies to the reduced dynamics when the description can be given in terms of time-local evolution equations, typically in the weak coupling regime, thus resulting in the Bloch-Redfield or Lindblad master equations [43–47]. In the limit of a high frequency driving, the Floquet approach can also be implemented beyond the weak coupling limit [48], by using the inverse frequency of modulations as a perturbation parameter.

In the present work we apply to the GME derived for the periodically driven spin-boson model the method presented in Ref. [49]. This method allows to find the asymptotic Floquet states of systems whose evolution is described by a master equations with memory kernels and is based on a so-called ‘embedding’ procedure. The embedding is performed by coupling the system to a set of non-physical variables, so that the resulting evolution equations governing the dynamics

in the enlarged space of variables are time-local. These equations have time-periodic coefficients and therefore are subjected to the standard Floquet theory. The projected solution in the physical subspace has the form requested by a generalization of the Floquet theorem [50] for systems with memory. We demonstrate that the method allows to investigate the spin dynamics in different dissipation regimes under periodical modulations with no restrictions on their amplitude or frequency.

II. EMBEDDING AND THE GENERALIZED FLOQUET THEORY

In this section we outline a generalization of the Floquet theorem [53, 54] to systems with memory [49]. Consider a periodically driven physical system described by the n -dimensional vector $\mathbf{x}(t)$ and governed by the time-nonlocal evolution equation

$$\dot{\mathbf{x}}(t) = \int_{t_0}^t dt' \mathbf{K}(t, t') \mathbf{x}(t') + \mathbf{z}(t) \quad (1)$$

with integrable memory kernel $\mathbf{K}(t, t')$. Assume that the inhomogeneous term vanishes asymptotically, i.e., $\lim_{t \rightarrow \infty} \mathbf{z}(t) = \mathbf{0}$, and that the kernel matrix is bi-periodic, namely, $\mathbf{K}(t + \mathcal{T}, t' + \mathcal{T}) = \mathbf{K}(t, t')$, where \mathcal{T} is the period of the driving. Under these conditions, in the limit $t \rightarrow \infty$, the action of $\mathcal{L}\{\mathbf{x}, t\}$, given by the right hand side of Eq. (1), commutes with that of the time-translation operator $\mathcal{S}_{\mathcal{T}}\{\mathbf{x}(t)\} = \mathbf{x}(t + \mathcal{T})$. Then, according to the generalized Floquet theory [50], the solution $\mathbf{x}(t)$ is formally expressed by

$$\mathbf{x}(t) = \mathbf{S}(t, t_0) e^{(t-t_0)\mathbf{F}} \mathbf{v}(t_0), \quad (2)$$

with $\mathbf{S}(t, t_0)$ a \mathcal{T} -periodic $n \times p$ matrix, \mathbf{F} a constant $p \times p$ matrix, and $\mathbf{v}(t_0)$ a p -dimensional constant vector, where $p \leq +\infty$.

In Ref. [49], we presented a method to find the asymptotic solution of Eq. (1). The method is based on the enlargement of the system state space by coupling \mathbf{x} to an auxiliary non-physical variable \mathbf{u} . The resulting extended system is described by the vector $\mathbf{v}^T = (x_1, \dots, x_n, u_1, u_2, \dots)$ which obeys a time-local equation. This equation is then subjected to the standard Floquet treatment [54]. By projecting the solution $\mathbf{v}(t)$ into the physical subspace, we find the solution for the original vector $\mathbf{x}(t)$.

We assume that the $n \times n$ kernel matrix in Eq. (1) can be expressed as (or approximated by) the following sum of complex matrices

$$\mathbf{K}(t, t') = \sum_{j=1}^k \Gamma_j e^{-\gamma_j(t-t')} \mathbf{E}_j(t) \mathbf{F}_j(t'), \quad (3)$$

with $\Gamma_j, \gamma_j \in \mathbb{C}$ and $\mathbf{E}_j(t) = \mathbf{E}_j(t + \mathcal{T})$, $\mathbf{F}_j(t) = \mathbf{F}_j(t + \mathcal{T})$ complex $n \times n$ matrices. This form is flexible enough to reproduce – at least approximatively, as we do below – a variety of memory kernels, including oscillatory ones [51].

With the kernel in the form of Eq. (3), the time evolution of the physical variable \mathbf{x} , Eq. (1), can be obtained by solving the following set of time-local equations [52]

$$\dot{\mathbf{x}}(t) = -\mathbf{H}(t)\mathbf{u}(t) \quad (4)$$

$$\dot{\mathbf{u}}(t) = -\mathbf{G}(t)\mathbf{x}(t) - \mathbf{A}\mathbf{u}(t), \quad (5)$$

where the n -dimensional vector \mathbf{x} is coupled to the auxiliary variable \mathbf{u} . Here we have introduced the matrices

$$\mathbf{H}(t) = \left(\Gamma_1 \mathbf{E}_1(t) \quad \dots \quad \Gamma_k \mathbf{E}_k(t) \right), \quad \mathbf{G}(t) = \begin{pmatrix} \mathbf{F}_1(t) \\ \vdots \\ \mathbf{F}_k(t) \end{pmatrix},$$

and $\mathbf{A} = \text{diag}(\gamma_1 \mathbf{1}^{n \times n}, \dots, \gamma_k \mathbf{1}^{n \times n})$.

(6)

These definitions entail that the vector of auxiliary variables has dimension $n \cdot k$.

Without loss of generality, we set $t_0 = 0$ from now on. To prove that Eqs. (4)-(5) are equivalent to Eq. (1), as far as the physical variable is concerned, we define $\mathbf{G}(t)\mathbf{x}(t) \equiv \mathbf{w}(t)$. Laplace transform of Eq. (5) yields $\mathbf{u}(\lambda) = [\lambda \mathbf{1} + \mathbf{A}]^{-1} \mathbf{u}(0) - [\lambda \mathbf{1} + \mathbf{A}]^{-1} \mathbf{w}(\lambda)$. Transforming back to the time domain, multiplying to the left by $-\mathbf{H}(t)$, and using Eq. (4), we recover Eq. (1) with

$$\mathbf{K}(t, t') = \mathbf{H}(t) e^{-\mathbf{A}(t-t')} \mathbf{G}(t'), \quad (7)$$

[which is equivalent to Eq. (3)] provided that

$$\mathbf{z}(t) = -\mathbf{H}(t) e^{-\mathbf{A}t} \mathbf{u}(0). \quad (8)$$

This requirement fixes the initial condition for the auxiliary vector $\mathbf{u}(t)$.

Equations (4)-(5) can be cast in the compact form

$$\dot{\mathbf{v}}(t) = \mathbf{M}(t)\mathbf{v}(t), \quad (9)$$

where $\mathbf{v}^\top = (x_1, \dots, x_n, u_1, \dots, u_{nk})$ is the p -dimensional state vector associated to the enlarged system, with $p = n + nk$, and $\mathbf{M}(t)$ is a $p \times p$ matrix with block structure

$$\mathbf{M}(t) = \begin{pmatrix} \mathbf{0} & -\mathbf{H}(t) \\ -\mathbf{G}(t) & -\mathbf{A} \end{pmatrix}, \quad (10)$$

where $\mathbf{0} \in \mathbb{R}^{n \times n}$. Note that having \mathcal{T} -periodic $\mathbf{H}(t)$ and $\mathbf{G}(t)$ entails \mathcal{T} -periodicity of $\mathbf{M}(t)$. Then, according to the Floquet theorem, Eq. (9) with initial condition $\mathbf{v}(t_0)$ has a formal solution whose projection in the physical subspace yields the form (2) [49, 50]. The asymptotic Floquet state of the original system at stroboscopic instances of time $t = s\mathcal{T}$, $s \in \mathbb{Z}$, is then given by the \mathbf{x} component of the extended vector \mathbf{v}^{as} , which is an invariant of the Floquet propagator $\mathbf{U}_{\mathcal{T}} = \hat{\mathbf{T}} \exp \left[\int_0^{\mathcal{T}} dt \mathbf{M}(t) \right]$, i.e., $\mathbf{U}_{\mathcal{T}} \mathbf{v}^{\text{as}}(s\mathcal{T}) = \mathbf{v}^{\text{as}}(s\mathcal{T})$ [46, 54]; here $\hat{\mathbf{T}}$ denotes the time-ordering operator.

III. THE PERIODICALLY DRIVEN SPIN-BOSON MODEL

Now we apply the method described in the previous section to a periodically modulated spin-boson model. In this model [1], a two-state system, the spin (or qubit), interacts with a dissipative environment represented by a set of independent bosonic modes of frequencies ω_i ('heat bath'). The strength of the coupling between the i -th mode and the two-state system is quantified by the frequency λ_i . According to the celebrated Caldeira-Leggett model [55], to which we include a time-dependent driving, the full Hamiltonian reads [23]

$$H(t) = -\frac{\hbar}{2} [\Delta \sigma_x + \varepsilon(t) \sigma_z] - \frac{\hbar}{2} \sigma_z \sum_i \lambda_i (a_i^\dagger + a_i) + \sum_i \hbar \omega_i a_i^\dagger a_i, \quad (11)$$

where Δ is the bare transition amplitude per unit time between the eigenstates $|\pm 1\rangle$ of the spin operator σ_z , and a_i (a_i^\dagger) is the annihilation (creation) operator of the i -th bosonic mode.

Following Ref. [43], we consider a monochromatic driving of amplitude ε_d and frequency Ω , with the time-dependent bias of the form

$$\varepsilon(t) = \varepsilon_0 + \varepsilon_d \cos(\Omega t). \quad (12)$$

This setting corresponds to the setup used in recent experiments [42].

The bath and its coupling to the two-state system can be fully specified by the spin-boson spectral density function $G(\omega) := \sum_i \lambda_i^2 \delta(\omega - \omega_i)$. For the bosonic heat bath, we assume the continuous Ohmic spectral density with a Drude cutoff [23]

$$G(\omega) = 2\alpha\omega(1 + \omega^2/\omega_c^2)^{-1}, \quad (13)$$

where the dimensionless parameter α quantifies the overall system-bath coupling and ω_c is the cutoff frequency. In a physical system where the spin dynamics occurs through tunneling transitions between sites at distance q_0 , the spin position operator is given by $\sigma_z q_0/2$. Let $\rho(t)$ denote the

spin density matrix. For a factorized system-bath initial condition at $t = 0$, with the heat bath initially being in the canonical thermal state, the exact dynamics of the population difference $\langle \sigma_z(t) \rangle = P_{+1}(t) - P_{-1}(t)$, where $P_{\pm 1} \equiv \langle \pm 1 | \rho(t) | \pm 1 \rangle$, is governed by the following GME:

$$\frac{d}{dt} \langle \sigma_z(t) \rangle = \int_0^t dt' [K^a(t, t') - K^s(t, t') \langle \sigma_z(t') \rangle], \quad (14)$$

where the symmetric (s) and antisymmetric (a) kernels – with respect to $\varepsilon(t)$ – have in general intricate path integral expressions [23, 43].

In the path integral picture, the Feynman-Vernon influence functional for the reduced system dynamics displays bath-induced, time-nonlocal interactions among the two-state transitions building up the paths. These interactions are mediated by the so-called pair interaction [23]

$$\begin{aligned} Q(t) &= Q'(t) + iQ''(t) \\ &= \int_0^\infty d\omega \frac{G(\omega)}{\omega^2} \left\{ \coth\left(\frac{\beta\hbar\omega}{2}\right) [1 - \cos(\omega t)] + i \sin(\omega t) \right\}, \end{aligned} \quad (15)$$

which is proportional to the second time integral of the bath correlation function. In terms of Matsubara frequencies $\nu_k = 2\pi k/\beta\hbar$ (with $k = 1, 2, \dots$), we get for the real part of the bath correlation function (see Ref. [31])

$$\begin{aligned} \frac{d^2}{dt^2} Q'(t) &= \int_0^\infty d\omega G(\omega) \coth\left(\frac{\beta\hbar\omega}{2}\right) \cos(\omega t) \\ &= c_0 e^{-\omega_c t} + \sum_{k=1}^\infty c_k e^{-\nu_k t}, \end{aligned} \quad (16)$$

and thus

$$Q(t) = \sum_{k=0}^\infty \frac{c_k}{\nu_k} \left[t - \frac{1 - e^{-\nu_k t}}{\nu_k} \right] + i\pi\alpha (1 - e^{-\omega_c t}), \quad (17)$$

where $\nu_0 \equiv \omega_c$ and where

$$\frac{c_k}{\nu_k} = 4\pi\alpha \frac{\omega_c^2}{\nu_k^2 - \omega_c^2} \quad (k \geq 1) \quad (18)$$

$$\text{and} \quad \frac{c_0}{\nu_0} = \pi\alpha\omega_c \cot\left(\frac{\beta\hbar\omega_c}{2}\right). \quad (19)$$

For sufficiently high temperature and cutoff frequency, $k_B T, \hbar\omega_c \gtrsim \hbar\Delta$, the real part $Q'(t)$ becomes a linear function of time and the imaginary part $Q''(t)$ is constant on a rather small time scale. In the path integral picture, this entails the decoupling of transitions which are distant in time. In this regime, the non-interacting blip approximation (NIBA), which accounts for only local-in-time correlations [1, 23], very well describes the dynamics of the population difference $\langle \sigma_z(t) \rangle$, as we show below. The NIBA is a nonperturbative approach with respect to the coupling

α : It is valid for the limit of strong coupling, when the stationary spin dynamics is fully incoherent. Besides, it is accurate down to low temperatures, for every α , provided that the bias is zero, $\varepsilon(t) = 0$.

Within the NIBA, the kernels $K^{s/a}(t, t')$ in Eq. (14) read [43]

$$\begin{aligned} K^s(t, t') &= h^s(t - t') \cos[\zeta(t, t')] \\ K^a(t, t') &= h^a(t - t') \sin[\zeta(t, t')] , \end{aligned} \quad (20)$$

with

$$\begin{aligned} h^s(t - t') &:= \Delta^2 e^{-Q'(t-t')} \cos[Q''(t - t')] \\ h^a(t - t') &:= \Delta^2 e^{-Q'(t-t')} \sin[Q''(t - t')] . \end{aligned} \quad (21)$$

The function $\zeta(t, t') = \int_{t'}^t dt'' \varepsilon(t'') = \xi(t) - \xi(t')$, where

$$\xi(t) = \varepsilon_0 t + \frac{\varepsilon_d}{\Omega} \sin(\Omega t) , \quad (22)$$

takes into account the modulations of the bias. Note that, in the absence of a time-dependent driving, i.e., $\varepsilon_d = 0$, the GME (14) with the NIBA kernels given by Eq. (20) acquires a convolutive character, namely the kernels depend exclusively on the difference $t - t'$.

By using the definition $\langle \sigma_z(t) \rangle = P_{+1}(t) - P_{-1}(t)$ and the conservation of probability $P_{+1}(t) + P_{-1}(t) = 1$, we can cast Eq. (14) into an equation describing the evolution of the population vector $\mathbf{p}^\top = (P_{+1}, P_{-1})$

$$\dot{\mathbf{p}}(t) = \int_0^t dt' \mathbf{K}(t, t') \mathbf{p}(t') , \quad (23)$$

which is of the form of Eq. (1) with dimension $n = 2$ and $\mathbf{z}(t) = 0$. This form is suitable to be generalized to the case of a multi-site (tight-binding) [43, 56] or multi-level [35, 57, 58] system. These generalizations fall under the domain of applicability of the present treatment. The 2×2 kernel matrix $\mathbf{K}(t, t')$ in Eq. (23) has elements

$$\begin{aligned} K_{-1+1}^{+1-1}(t, t') &= \frac{1}{2} [K^s(t, t') \pm K^a(t, t')] \\ K_{-1-1}^{+1+1}(t, t') &= -K_{+1-1}^{-1+1}(t, t') , \end{aligned} \quad (24)$$

and can thus be written as

$$\mathbf{K}(t, t') = \frac{1}{2} \sum_{j=s,a} h^j(t - t') \mathbf{E}_j(t) \mathbf{F}_j(t') . \quad (25)$$

The effect of the driving is encapsulated in the time-dependent matrices $\mathbf{E}_j(t)$ and $\mathbf{F}_j(t)$ reading

$$\begin{aligned} \mathbf{E}_s(t) &= \begin{pmatrix} \cos[\xi(t)] & \sin[\xi(t)] \\ -\cos[\xi(t)] & -\sin[\xi(t)] \end{pmatrix} & \mathbf{E}_a(t) &= \begin{pmatrix} \sin[\xi(t)] & \cos[\xi(t)] \\ -\sin[\xi(t)] & -\cos[\xi(t)] \end{pmatrix} \\ \mathbf{F}_s(t) &= \begin{pmatrix} -\cos[\xi(t)] & \cos[\xi(t)] \\ -\sin[\xi(t)] & \sin[\xi(t)] \end{pmatrix} & \mathbf{F}_a(t) &= \begin{pmatrix} \cos[\xi(t)] & \cos[\xi(t)] \\ -\sin[\xi(t)] & -\sin[\xi(t)] \end{pmatrix}, \end{aligned} \quad (26)$$

where the function $\xi(t)$ has been defined in Eq. (22).

In order to complete the embedding, we need to cast the kernel matrix in the form prescribed by Eq. (3). To this aim, we approximate the two functions $h^{s/a}(t)$ introduced in Eq. (21) as the following sums of oscillating exponentials

$$\begin{aligned} h^s(t) &\simeq c_1 e^{-c_2 t} \cos(c_3 t) + c_4 e^{-c_5 t} \\ &\equiv 2 \sum_{j=1}^3 \Gamma_j e^{-\gamma_j t} \\ h^a(t) &\simeq e^{-d_1 t} \sin(d_2 t) + d_3 \left(e^{-d_4 t} - e^{-d_5 t} \right) \\ &\equiv 2 \sum_{j=4}^7 \Gamma_j e^{-\gamma_j t}. \end{aligned} \quad (27)$$

This yields the complex coefficients Γ_j and γ_j in Eq. (3). Indeed, by comparing with Eq. (25) we find

$$\mathbf{K}(t, t') \simeq \sum_{j=1}^7 \Gamma_j e^{-\gamma_j(t-t')} \mathbf{E}_j(t) \mathbf{F}_j(t'), \quad (28)$$

with

$$\begin{aligned} \Gamma_1 = \Gamma_2 = c_1/4, \quad \Gamma_3 = c_4/2, \quad \Gamma_4 = -i/4, \quad \Gamma_5 = +i/4, \quad \Gamma_6 = +d_3/2, \quad \Gamma_7 = -d_3/2 \\ \gamma_1 = c_2 - ic_3, \quad \gamma_2 = c_2 + ic_3, \quad \gamma_3 = c_5, \quad \gamma_4 = d_1 - id_2, \quad \gamma_5 = d_1 + id_2, \quad \gamma_6 = d_4, \quad \gamma_7 = d_5 \end{aligned} \quad (29)$$

and

$$\begin{aligned} \mathbf{E}_1(t) = \mathbf{E}_2(t) = \mathbf{E}_3(t) = \mathbf{E}_s(t), \quad \mathbf{E}_4(t) = \mathbf{E}_5(t) = \mathbf{E}_6(t) = \mathbf{E}_7(t) = \mathbf{E}_a(t) \\ \mathbf{F}_1(t) = \mathbf{F}_2(t) = \mathbf{F}_3(t) = \mathbf{F}_s(t), \quad \mathbf{F}_4(t) = \mathbf{F}_5(t) = \mathbf{F}_6(t) = \mathbf{F}_7(t) = \mathbf{F}_a(t). \end{aligned} \quad (30)$$

Once that the physical parameters of the problem are fixed, the coefficients $c_j, d_j \in \mathbb{R}$ can be obtained upon a fitting procedure, see Appendix B, by using the approximated expressions (27) as fitting functions. The coefficients, in turn, produce the complex coefficients γ_j and Γ_j through

Eq. (29). Applying to the present case the general rule, the dimension of the embedded system is $n + nk = 16$ with $n = 2$, the dimension of the physical variable \mathbf{p} , and $nk = 14$ the dimension of the auxiliary variable \mathbf{u} , being $k = 7$ (see Eq. (28)). The extended system is thus described by $\mathbf{v}^\top = (P_{+1}, P_{-1}, u_1, \dots, u_{14})$. Its asymptotic state is invariant under the action of the Floquet propagator $\mathbf{U}_\mathcal{T}$. The latter is in practice constructed as follows. Its columns are the one-period propagated elements of the canonical basis of \mathbb{R}^{16} $(1, 0, \dots, 0), (0, 1, \dots, 0), \dots, (0, 0, \dots, 1)$. The propagation is performed via the time-local matrix equation (9) by using a 4-th order Runge-Kutta scheme with the rather small time step $\delta = \mathcal{T}/10^4$, where $\mathcal{T} = 2\pi/\Omega$. The invariant vector \mathbf{v}^{as} is the eigenvector of $\mathbf{U}_\mathcal{T}$ corresponding to eigenvalue 1. The asymptotic Floquet state on a time span of one period is then obtained by propagating for one period the extended system, with \mathbf{v}^{as} as initial condition.

In concluding the present section we note that if the driving period Ω is a multiple of the static bias ε_0 , then the extended system has the period $\mathcal{T} = 2\pi/\Omega$ of the driving. Moreover, if the ratio Ω/ε_0 is a rational number then the periodicity of the extended system is $\mathcal{T} = m2\pi/\varepsilon_0$, where m is the minimum integer such that the ratio $m\Omega/\varepsilon_0$, is also an integer. On the other hand, if the frequencies ε_0 and Ω are not commensurate, then the embedding procedure still yields a time-local system but with non-periodic coefficients; such systems do not allow for the Floquet treatment. However, these considerations hold for the extended system while the physical degrees of freedom have, asymptotically, the periodicity of the driving, independently of the values of static bias and driving frequency.

IV. RESULTS

In the present section, we calculate asymptotic states of the driven spin-boson model for the three values of coupling strength $\alpha = 0.05, 0.2, \text{ and } 0.6$ and different values of static bias ε_0 , driving amplitude ε_d , and frequency Ω . All physical parameters are scaled with the frequency Δ , the bare transition amplitude per unit time of the two-state system; see Eq. (11). The results presented are obtained for temperature $T = 0.7 \hbar\Delta/k_B$ and Drude cutoff frequency $\omega_c = 5 \Delta$. For each value of α , the coefficients of the embedding are determined by numerically optimizing the approximated expressions for $h^{s/a}(t)$, Eq. (27), against the numerical evaluations of the corresponding exact expressions in Eq. (21) (see Appendix B).

In Fig. 1, we depict the physical part of the asymptotic Floquet states of the extended system, namely the population difference $\langle\sigma_z(t)\rangle$ of the two-state system, at zero static bias, $\varepsilon_0 = 0$,

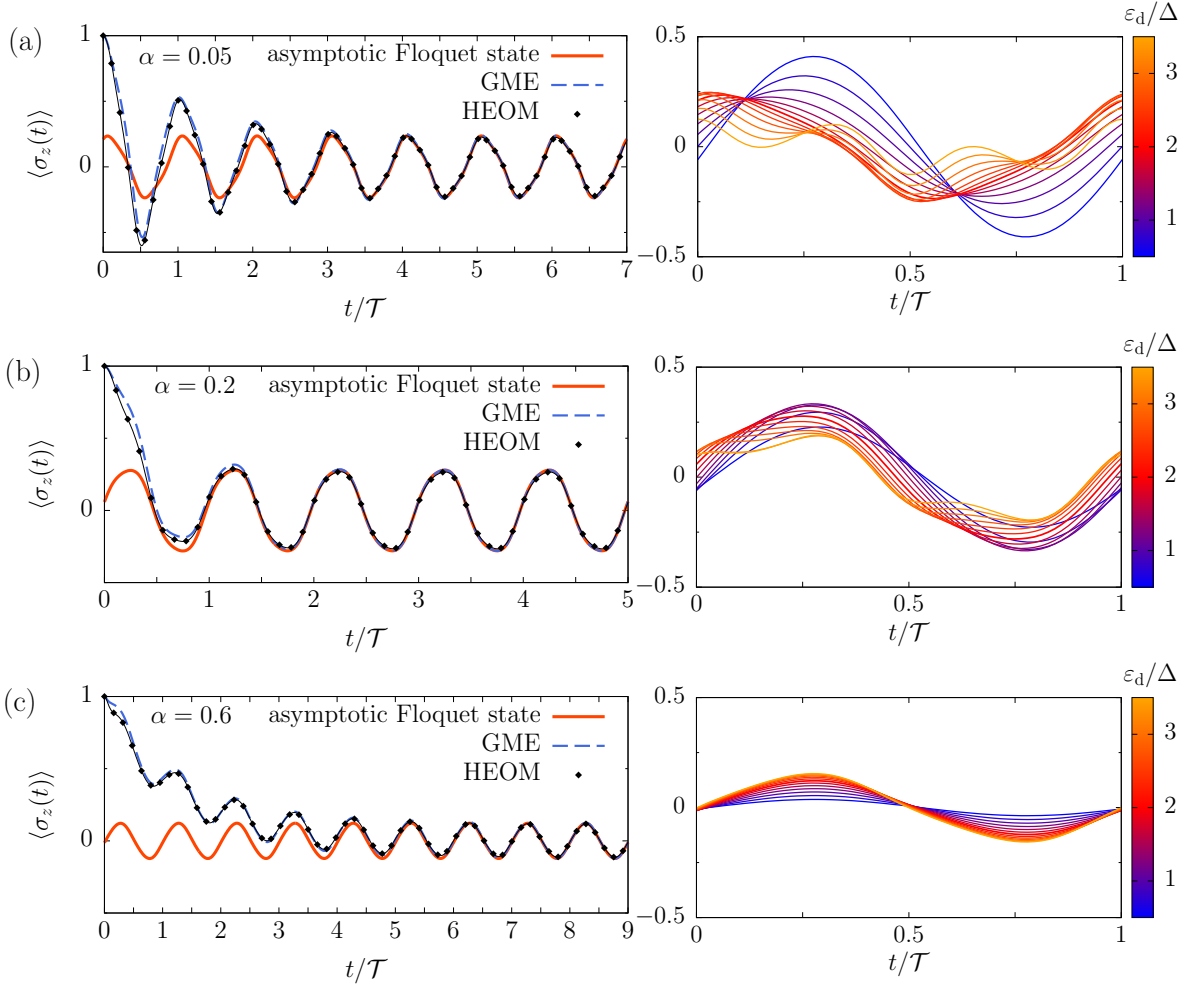


FIG. 1. Asymptotic Floquet states of the driven spin-boson model, Eq. (11), for different coupling strengths and modulation amplitudes. Left panels: Asymptotic population difference $\langle \sigma_z(t) \rangle = P_{+1}(t) - P_{-1}(t)$ vs time at fixed driving amplitude $\varepsilon_d = 2 \Delta$. The populations $P_{\pm 1}(t)$ are the physical components of the extended system obeying the time local equation (9) (solid lines). A comparison is made with the corresponding propagated solutions of the GME (14) (dashed lines) and the converged numerically exact HEOM (diamonds), starting with $P_{+1}(0) = 1$. Right panels: Asymptotic Floquet states for different values of the drive amplitude ε_d evaluated for the same coupling strengths α as in the corresponding left panels. The thick red curves depict the same asymptotic dynamics as those in the corresponding left panels. Note that, for different values of the spin-boson coupling strength α , the maximum amplitude of the oscillations is reached at a different driving amplitude ε_d . Fixed parameters are: Static bias $\varepsilon_0 = 0$, driving frequency $\Omega = \Delta$, temperature $T = 0.7 \hbar \Delta / k_B$, and Drude cutoff $\omega_c = 5 \Delta$. Time is in units of the driving period $\mathcal{T} = 2\pi/\Omega$.

and at fixed driving frequency $\Omega = \Delta$. This is done for the three values of coupling strength considered and by changing the drive amplitude. In the left panels we show, for $\varepsilon_d = 2 \Delta$, the asymptotic Floquet states over multiple driving periods along with the transient dynamics, as

obtained by integrating the NIBA generalized master equation (14) (see Appendix A for details) with initial condition $\langle \sigma_z(0) \rangle = 1$. This provides information on the time scales of relaxation to the asymptotic, time-periodic dynamics at different dissipation regimes and also certifies that the embedding procedure renders correctly the dynamics obtained from the GME. We note that, in the asymptotic limit, the results of the integration of the GME and of the Floquet solutions coincide perfectly, notwithstanding that the decomposition of the memory kernel employed in the embedding is only approximate, thus confirming the flexibility of the embedding method described in Sec. II. We benchmark the NIBA results with the numerically exact approach of hierarchical equations of motion (HEOM) (see Appendix A), obtaining reasonable agreement, even for $\varepsilon(t) \neq 0$, in all of the dissipation regimes.

The right panels of Fig. 1 depict the asymptotic Floquet states over a single driving period for driving strengths ε_d in the range $[0.5 \Delta, 3.5 \Delta]$. Note that the maximum amplitude of the oscillations is reached at different strengths for different values of α and that, in general, a large value of the coupling tends to suppress the higher harmonics which are most clearly visible for $\alpha = 0.05$ in the nonlinear driving regime, i.e. when the condition $\varepsilon_d/\Omega \ll 1$ is not met.

The same behavior is displayed by the system also in the biased case, as depicted in the right panels of Fig. 2, where the Floquet asymptotic states over a time span of one driving period are shown with $\varepsilon_0 = \Delta$, for driving strengths ε_d in the range $[0.25 \Delta, 6.25 \Delta]$. We note that, as ε_d dominates over the static bias, the symmetry of the oscillations around $\langle \sigma_z \rangle = 0$ tends to be restored. However, an increase of the coupling α tends to localize the spin state in the energetically more favourable state $|+1\rangle$, thus counteracting the effect of the time-periodic component of the driving.

Figure 2 also depicts the asymptotic states at finite static bias (left panels), $\varepsilon_0 = 0.5 \Delta$, for three values of the frequency Ω . Note that, for $\alpha = 0.05$, Fig. 2(a), even if the bias is positive, at the intermediate value of frequency, $\Omega = 1.5 \Delta$, the population difference mostly assumes negative values. This can be accounted for in terms of a negative effective bias ε_{eff} , implicitly defined by the detailed balance relation [42, 43] $K^f = K^b \exp(\beta \hbar \varepsilon_{\text{eff}})$, where $K^{f(b)} = (1/\mathcal{T}) \int_0^{\mathcal{T}} dt \int_0^{\infty} d\tau K_{(-1+1)}^{+1-1}(t, t - \tau)$ are the static rates obtained by averaging over the driving period the time-integrated kernel matrix elements.

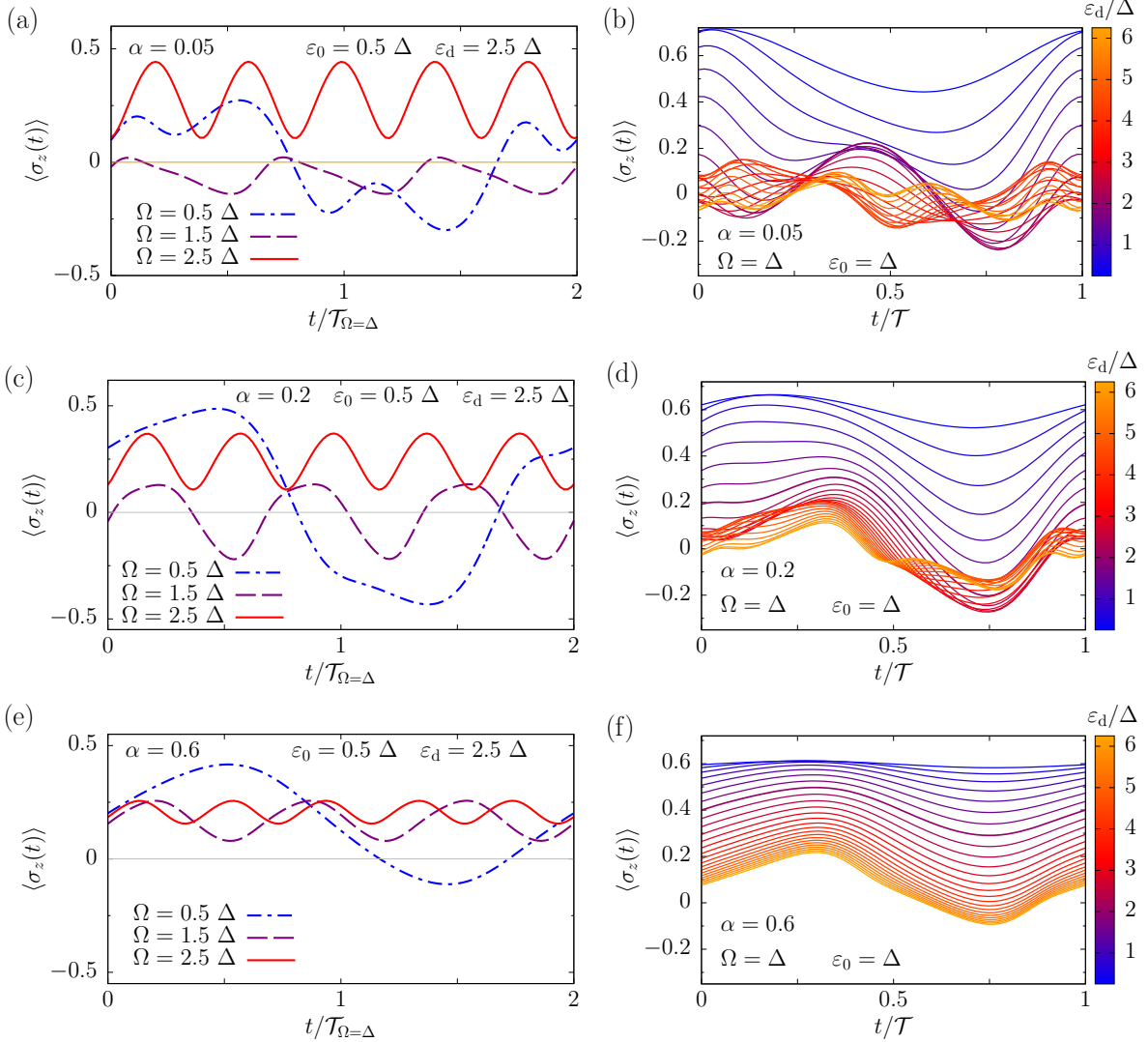


FIG. 2. Asymptotic Floquet states of the driven spin-boson model (11) with finite static bias. For each of the three values of the coupling strength α , on the left panels the driving frequency Ω is varied at fixed driving strength $\varepsilon_d = 2.5 \Delta$ and for $\varepsilon_0 = 0.5 \Delta$, while the right panels show the asymptotic states at fixed frequency and constant static bias $\Omega = \varepsilon_0 = \Delta$ for different driving amplitudes. Temperature and Drude cutoff are $T = 0.7 \hbar\Delta/k_B$ and $\omega_c = 5 \Delta$, respectively. Time is in units of the driving period $\mathcal{T} = 2\pi/\Omega$ with $\Omega = \Delta$.

V. CONCLUSIONS AND OUTLOOK

In this work, we used the method developed in Ref. [49] to find the asymptotic Floquet states of time-nonlocal evolution equations, to the periodically driven spin-boson model beyond the perturbative regime of coupling with the bosonic heat bath.

The method rests on reshaping the memory kernel into a specific form, which is suitable to

model memory kernels which decay monotonously or with oscillations. This representation allows to embed the system dynamics into an enlarged state space, by coupling the actual physical variables to a set of auxiliary non-physical variables. The dynamics of the so-obtained enlarged system is governed by a time-local equation to which the standard Floquet formalism applies.

We considered temperature/coupling regimes where the non-interacting blip approximation of the path integral expression for the reduced dynamics describes satisfactorily the driven spin-boson model, as we demonstrate upon comparison with evaluations of the dynamics by using converged hierarchical equations of motions. In particular, the probabilities associated to the spin states are given by a generalized master equation displaying a memory kernel which accounts for the effects of the environment and of the driving. By using an optimization procedure, we performed an approximate embedding and find the asymptotic Floquet states of the spin dynamics as the projection of the Floquet states of the enlarged system onto the physical subspace. We illustrated this idea by calculating asymptotic Floquet states in different dissipation and driving regimes, both for the unbiased and biased system.

Our results demonstrate, see Fig 1, that the proposed method still performs well in the cases where the expression in Eq. (3) is employed with a finite number of terms to approximate the memory kernel. Finally, the study of the driven dynamics of the spin-boson model performed in the present work can be generalized to multi-site or multi-level systems subjected to periodical modulations [35, 43, 56–58].

ACKNOWLEDGEMENTS

S. D. and P. H. acknowledge the support by the Russian Science Foundation, Grant No. 15-12-20029 (S.D.) and by the Deutsche Forschungsgemeinschaft (DFG) via the grants DE1889/1-1 (S.D.) and HA1517/35-1 (P.H.).

Appendix A: HEOM and details of the simulations

Consider an open system of effective mass M coupled to a heat bath with Ohmic-Drude spectral density function and cutoff frequency ω_c ,

$$J(\omega) = \eta\omega(1 + \omega^2/\omega_c^2)^{-1}, \quad (\text{A1})$$

where $\eta = M\gamma$ is the viscosity parameter and γ the friction parameter with dimensions of frequency. Specialization to a two-state system characterized by tunneling between sites separated by the

distance $q_0 = 2d$ yields [23]:

$$\alpha = \frac{\eta q_0^2}{2\pi\hbar} = \frac{2}{\pi}\eta\frac{d^2}{\hbar}. \quad (\text{A2})$$

We set $d = 1$, in units of $(M\Delta/\hbar)^{-1/2}$, so that the position eigenvalues are identified with the eigenvalues of σ_z .

In the HEOM approach [29–31], the time evolution of an open system interacting through the operator V (in the present case $V \equiv \sigma_z$) with a harmonic heat bath is governed by a set of coupled time-local evolution equations for a set of density matrices $\{\rho_{n,\mathbf{j}}(t)\}$ of which only $\rho_{0,\mathbf{0}}(t)$ describes the actual physical system, while the others are auxiliary, non-physical density matrices. This approach exploits the fact that, for a Ohmic spectral density with Drude cutoff, the bath correlation function

$$L(t) = \frac{1}{\pi} \int_0^\infty d\omega J(\omega) \left[\coth\left(\frac{\beta\hbar\omega}{2}\right) \cos(\omega t) - i \sin(\omega t) \right] \quad (\text{A3})$$

can be expressed as a series over the Matsubara frequencies $\nu_k = 2\pi k/(\hbar\beta)$, as done in Eq. (16). The Padé spectrum decomposition allows for an efficient truncation of this series to the first M terms [59], even when the temperature is not much larger than the characteristic frequency Δ of the system, as in our case where $k_B T < \hbar\Delta$. The hierarchy of equations reads

$$\begin{aligned} \dot{\rho}_{n,\mathbf{j}}(t) = & - \left[\frac{i}{\hbar} H(t)^\times + n\omega_c + \sum_{k=1}^M j_k \nu_k + \left(g - \sum_{k=1}^M f_k \right) V^\times V^\times \right] \rho_{n,\mathbf{j}}(t) \\ & - i V^\times \rho_{n+1,\mathbf{j}}(t) - n\omega_c (\theta V^\circ + i\varphi V^\times) \rho_{n-1,\mathbf{j}}(t) \\ & - i \sum_{k=1}^M V^\times \rho_{n,\mathbf{j}_{k+}}(t) - i \sum_{k=1}^M j_k \nu_k f_k V^\times \rho_{n,\mathbf{j}_{k-}}(t), \end{aligned} \quad (\text{A4})$$

where $\mathcal{O}^\times \rho := [\mathcal{O}, \rho]$ and $\mathcal{O}^\circ \rho := \{\mathcal{O}, \rho\}$, for a given operator \mathcal{O} , and where the following quantities have been introduced

$$\theta = \frac{\eta\omega_c}{2}, \quad \varphi = \theta \cot\left(\frac{\beta\hbar\omega_c}{2}\right), \quad g = \frac{\eta}{\hbar\beta} - \varphi, \quad \text{and} \quad f_k = \frac{\eta}{\hbar\beta} \frac{2\omega_c^2}{\nu_k^2 - \omega_c^2}. \quad (\text{A5})$$

It is understood that the contributing density matrices have both n and all of the components of the vector index $\mathbf{j} = (j_1, \dots, j_k, \dots, j_M)$ nonnegative. Moreover $\mathbf{j}_{k\pm}$ is a short-hand notation for $(j_1, \dots, j_k \pm 1, \dots, j_M)$. The terminators of the hierarchy of equations (A4) are identified by the condition $n + \sum_{k=1}^M j_k = N$, for some $N \gg \omega_0/\min(\omega_c, \nu_1)$, and read

$$\dot{\rho}_{n,\mathbf{j}}(t) \simeq - \left[\frac{i}{\hbar} H(t)^\times + \left(g - \sum_{k=1}^M f_k \right) V^\times V^\times \right] \rho_{n,\mathbf{j}}(t) \quad (\text{A6})$$

In Figs. 1 and 3, NIBA results for the reduced dynamics are compared with those from converged HEOM for the driven and non-driven case, respectively. Simulations performed by implementing

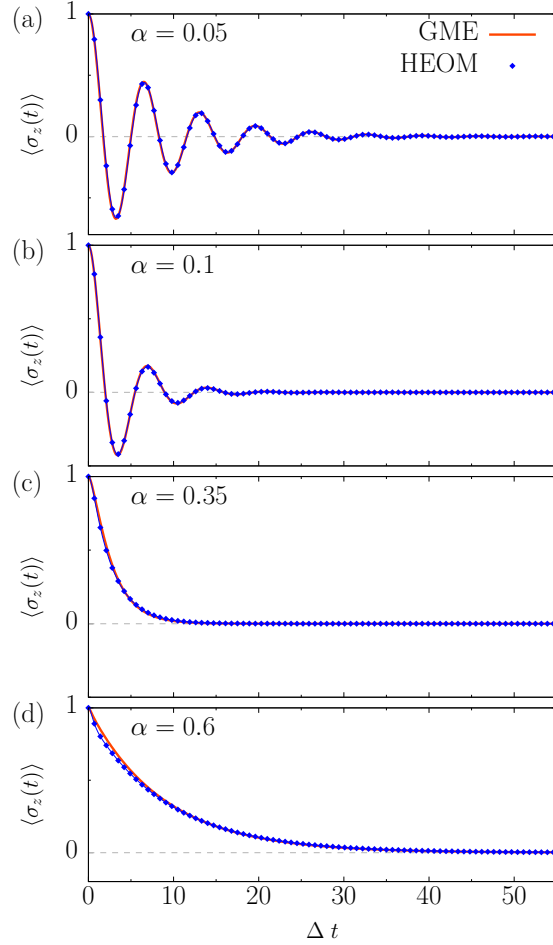


FIG. 3. Comparison between the results of the GME (14) (solid lines) and converged HEOM (diamonds) in the unbiased, static case $\varepsilon(t) = 0$, for different values of the coupling strength α . Temperature and cutoff frequency are $T = 0.7 \hbar\Delta/k_B$ and $\omega_c = 5 \Delta$, respectively.

the HEOM with Padé spectrum decomposition of the bath correlation function are converged with $M = 3$ and $N = 10$, for all the parameters considered. The propagation of the HEOM is obtained by using a second order Runge-Kutta scheme with time step $\delta t = 5 \times 10^{-4} \Delta^{-1}$. The GME (14) is propagated by using the trapezoid rule for the integral and the forward finite difference for the time derivative, according to the simple implicit scheme described in [58] for a multi-level generalization of the spin-boson model. The time step is $\delta t = 5 \times 10^{-3} \Delta^{-1}$.

Appendix B: Fits to kernels

In Fig. 4 we show the optimized curves corresponding to the approximate expressions in Eq. (27) with coefficients extracted by fitting the numerically exact evaluations of the functions in Eq. (21).

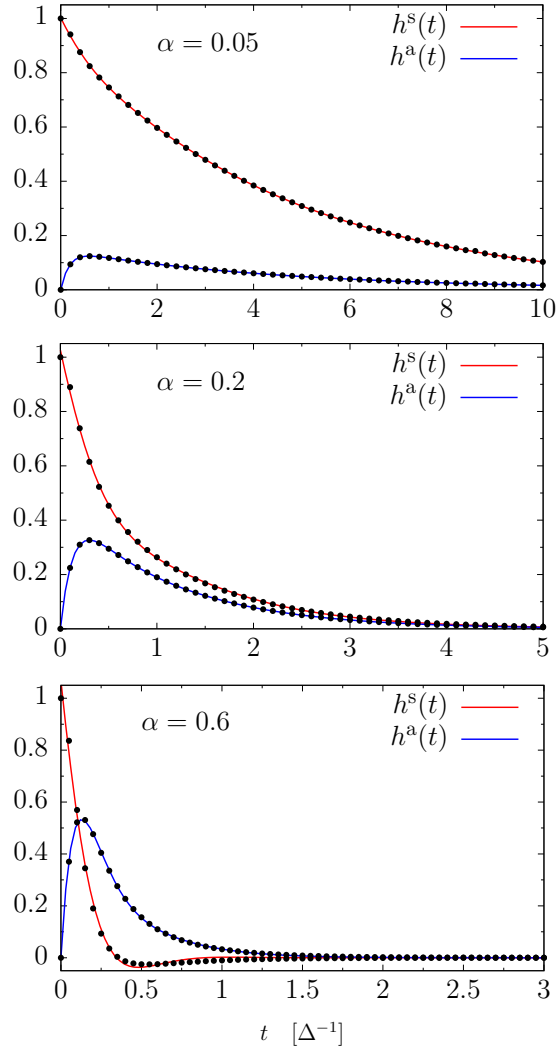


FIG. 4. Numerical fits of the functions $h^{s/a}(t)$ defined in Eq. (21) performed by using the approximated expressions in Eq. (27). The coefficients of these approximated expressions (solid lines) are determined by fitting the numerically exact evaluations (bullets). The latter are performed by truncating the sum for $Q'(t)$ to the first 4000 terms (see Eq. (17)). Temperature and Drude cutoff frequency are $T = 0.7 \hbar\Delta/k_B$ and $\omega_c = 5 \Delta$, respectively.

Note that, as these functions do not depend on the driving, the results shown in the present work required three sets of coefficients, corresponding to the three panels in Fig. 4.

-
- [1] A. J. Leggett, S. Chakravarty, A. T. Dorsey, M. P. A. Fisher, A. Garg, and W. Zwerger, “Dynamics of the dissipative two-state system,” *Rev. Mod. Phys.* **59**, 1–85 (1987); **67**, 725(E) (1995) .
- [2] R. I. Cukier and M. Morillo, “Solvent effects on proton transfer reactions,” *J. Chem. Phys.* **91**, 857–863 (1989), doi: 10.1063/1.457137.
- [3] J. Stockburger and C. H. Mak, “A dynamical theory of electron transfer: Crossover from weak to strong electronic coupling,” *J. Chem. Phys.* **105**, 8126–8135 (1996).
- [4] M. Thorwart, J. Eckel, J.H. Reina, P. Nalbach, and S. Weiss, “Enhanced quantum entanglement in the non-Markovian dynamics of biomolecular excitons,” *Chem. Phys. Lett.* **478**, 234–237 (2009).
- [5] S. F. Huelga and M. B. Plenio, “Vibrations, quanta and biology,” *Contemp. Phys.* **54**, 181–207 (2013).
- [6] S. Han, J. Lapointe, and J. E. Lukens, “Observation of incoherent relaxation by tunneling in a macroscopic two-state system,” *Phys. Rev. Lett.* **66**, 810–813 (1991).
- [7] J. Leppäkangas, J. Braumüller, M. Hauck, J.-M. Reiner, I. Schwenk, S. Zanker, L. Fritz, A. V. Ustinov, M. Weides, and M. Marthaler, “Quantum simulation of the spin-boson model with a microwave circuit,” arXiv:1711.07463 (2017).
- [8] H.-P. Breuer and F. Petruccione, *The theory of open quantum systems* (Oxford University Press, 2002).
- [9] D. P. DiVincenzo and D. Loss, “Rigorous Born approximation and beyond for the spin-boson model,” *Phys. Rev. B* **71**, 035318 (2005).
- [10] C. J. Lindner and H. Schoeller, “Dissipative quantum mechanics beyond Bloch-Redfield: A consistent weak-coupling expansion of the ohmic spin boson model at arbitrary bias,” arXiv:1802.09846 (2018).
- [11] J. T. Stockburger and H. Grabert, “Exact c -Number Representation of Non-Markovian Quantum Dissipation,” *Phys. Rev. Lett.* **88**, 170407 (2002).
- [12] P. P. Orth, A. Imambekov, and K. Le Hur, “Nonperturbative stochastic method for driven spin-boson model,” *Phys. Rev. B* **87**, 014305 (2013).
- [13] H. D. Meyer, U. Manthe, and L. S. Cederbaum, “The multi-configurational time-dependent Hartree approach,” *Chem. Phys. Lett.* **165**, 73–78 (1990).
- [14] H. Wang and M. Thoss, “Multilayer formulation of the multiconfiguration time-dependent Hartree theory,” *The Journal of Chemical Physics*, *J. Chem. Phys.* **119**, 1289–1299 (2003).
- [15] D. P. S. McCutcheon, N. S. Dattani, E. M. Gauger, B. W. Lovett, and A. Nazir, “A general approach to quantum dynamics using a variational master equation: Application to phonon-damped Rabi rotations in quantum dots,” *Phys. Rev. B* **84** (2011).
- [16] I. de Vega and D. Alonso, “Dynamics of non-Markovian open quantum systems,” *Rev. Mod. Phys.* **89**, 015001 (2017).
- [17] R. Bulla, T. A. Costi, and T. Pruschke, “Numerical renormalization group method for quantum impurity systems,” *Rev. Mod. Phys.* **80**, 395–450 (2008).

- [18] A. Alvermann and H. Fehske, “Sparse Polynomial Space Approach to Dissipative Quantum Systems: Application to the Sub-Ohmic Spin-Boson Model,” *Phys. Rev. Lett.* **102**, 150601 (2009).
- [19] A. W. Chin, Á. Rivas, S. F. Huelga, and M. B. Plenio, “Exact mapping between system-reservoir quantum models and semi-infinite discrete chains using orthogonal polynomials,” *J. Math. Phys.* **51**, 092109 (2010).
- [20] R. Martinazzo, B. Vacchini, K. H. Hughes, and I. Burghardt, “Communication: Universal Markovian reduction of Brownian particle dynamics,” *J. Chem. Phys.* **134**, 011101 (2011).
- [21] J. Iles-Smith, N. Lambert, and A. Nazir, “Environmental dynamics, correlations, and the emergence of noncanonical equilibrium states in open quantum systems,” *Phys. Rev. A* **90**, 032114 (2014).
- [22] I. de Vega and M.-C. Bañuls, “Thermofield-based chain-mapping approach for open quantum systems,” *Phys. Rev. A* **92**, 052116 (2015).
- [23] U. Weiss, *Quantum Dissipative Systems* (World Scientific, Singapore, 2012, 4th ed.).
- [24] R. Egger and U. Weiss, “Quantum Monte Carlo simulation of the dynamics of the spin-boson model,” *Z. Physik B* **89**, 97–107 (1992).
- [25] R. Egger and C. H. Mak, “Low-temperature dynamical simulation of spin-boson systems,” *Phys. Rev. B* **50**, 15210–15220 (1994).
- [26] D. Kast and J. Ankerhold, “Persistence of Coherent Quantum Dynamics at Strong Dissipation,” *Phys. Rev. Lett.* **110**, 010402 (2013).
- [27] D. E. Makarov and N. Makri, “Path integrals for dissipative systems by tensor multiplication. Condensed phase quantum dynamics for arbitrarily long time,” *Chem. Phys. Lett.* **221**, 482–491 (1994).
- [28] N. Makri, “Numerical path integral techniques for long time dynamics of quantum dissipative systems,” *Journal of Mathematical Physics*, *J. Math. Phys.* **36**, 2430–2457 (1995).
- [29] Y. Tanimura and R. Kubo, “Time Evolution of a Quantum System in Contact with a Nearly Gaussian-Markoffian Noise Bath,” *J. Phys. Soc. Jpn.* **58**, 101–114 (1989).
- [30] A. Ishizaki and Y. Tanimura, “Quantum Dynamics of System Strongly Coupled to Low-Temperature Colored Noise Bath: Reduced Hierarchy Equations Approach,” *J. Phys. Soc. Jpn.* **74**, 3131–3134 (2005).
- [31] Y. Tanimura, “Stochastic Liouville, Langevin, Fokker-Planck, and Master Equation Approaches to Quantum Dissipative Systems,” *J. Phys. Soc. Jpn.* **75**, 082001 (2006).
- [32] J. M. Moix and J. Cao, “A hybrid stochastic hierarchy equations of motion approach to treat the low temperature dynamics of non-Markovian open quantum systems,” *J. Chem. Phys.* **139**, 134106 (2013).
- [33] L. Hartmann, I. Goychuk, M. Grifoni, and P. Hänggi, “Driven tunneling dynamics: Bloch-Redfield theory versus path-integral approach,” *Phys. Rev. E* **61**, R4687–R4690 (2000) .
- [34] F. Nesi, E. Paladino, M. Thorwart, and M. Grifoni, “Spin-boson dynamics beyond conventional perturbation theories,” *Phys. Rev. B* **76**, 155323 (2007).
- [35] L. Magazzù, D. Valenti, B. Spagnolo, and M. Grifoni, “Dissipative dynamics in a quantum bistable system: Crossover from weak to strong damping,” *Phys. Rev. E* **92**, 032123 (2015).

- [36] I. Chiorescu, Y. Nakamura, C. J. P. M. Harmans, and J. E. Mooij, “Coherent Quantum Dynamics of a Superconducting Flux Qubit,” *Science* **299**, 1869 (2003).
- [37] P. Forn-Díaz, J. J. Garcia-Ripoll, B. Peropadre, J. L. Orgiazzi, M. A. Yurtalan, R. Belyansky, C. M. Wilson, and A. Lupascu, “Ultrastrong coupling of a single artificial atom to an electromagnetic continuum in the nonperturbative regime,” *Nat. Phys.* **13**, 39–43 (2017).
- [38] J. Q. You and F. Nori, “Atomic physics and quantum optics using superconducting circuits,” *Nature* **474**, 589 (2011).
- [39] M. H. Devoret and R. J. Schoelkopf, “Superconducting Circuits for Quantum Information: An Outlook,” *Science* **339**, 1169 (2013).
- [40] G. Wendin, “Quantum information processing with superconducting circuits: a review,” *Rep. Prog. Phys.* **80**, 106001 (2017).
- [41] D. Roy, C. M. Wilson, and O. Firstenberg, “Colloquium: Strongly interacting photons in one-dimensional continuum,” *Rev. Mod. Phys.* **89**, 021001 (2017).
- [42] L. Magazzù, P. Forn-Díaz, R. Belyansky, J.-L. Orgiazzi, M. A. Yurtalan, M. R. Otto, A. Lupascu, C. M. Wilson, and M. Grifoni, “Probing the strongly driven spin-boson model in a superconducting quantum circuit,” *Nat. Commun.* **9**, 1403 (2018).
- [43] M. Grifoni and P. Hänggi, “Driven quantum tunneling,” *Phys. Rep.* **304**, 229–354 (1998).
- [44] J. Hausinger and M. Grifoni, “Dissipative two-level system under strong ac driving: A combination of Floquet and Van Vleck perturbation theory,” *Phys. Rev. A* **81**, 022117 (2010).
- [45] T. Shirai, J. Thingna, T. Mori, S. Denisov, P. Hänggi, and S. Miyashita, “Effective Floquet–Gibbs states for dissipative quantum systems,” *New J. Phys.* **18**, 053008 (2016).
- [46] M. Hartmann, D. Poletti, M. Ivanchenko, S. Denisov, and P. Hänggi, “Asymptotic Floquet states of open quantum systems: the role of interaction,” *New J. Phys.* **19**, 083011 (2017).
- [47] V. M. Bastidas, T. H. Kyaw, J. Tangpanitanon, G. Romero, L.-C. Kwek, and D. G. Angelakis, “Floquet stroboscopic divisibility: coherence preservation in non-Markovian dynamics,” *arXiv:1707.04423* (2017).
- [48] S. Restrepo, J. Cerrillo, V. M. Bastidas, D. G. Angelakis, and T. Brandes, “Driven Open Quantum Systems and Floquet Stroboscopic Dynamics,” *Phys. Rev. Lett.* **117**, 250401 (2016); *Phys. Rev. Lett.* **118**, 049903 (2017).
- [49] L. Magazzù, S. Denisov, and P. Hänggi, “Asymptotic Floquet states of non-Markovian systems,” *Phys. Rev. A* **96**, 042103 (2017).
- [50] F. L. Traversa, M. Di Ventura, and F. Bonani, “Generalized Floquet Theory: Application to Dynamical Systems with Memory and Bloch’s Theorem for Nonlocal Potentials,” *Phys. Rev. Lett.* **110**, 170602 (2013).
- [51] G. Beylkin and L. Monzón, “On approximation of functions by exponential sums,” *Appl. Comput. Harmon. A.* **19**, 17–48 (2005).

- [52] R. Kupferman, “Fractional Kinetics in Kac–Zwanzig Heat Bath Models,” *J. Stat. Phys.* **114**, 291–326 (2004).
- [53] G. Floquet, *Ann. Sci. Ec. Norm. Sup.* **12**, 47 (1883).
- [54] V. A. Yakubovich and V. M. Starzhinskii, *Linear Differential Equations with Periodic Coefficients* (Wiley, New York, 1975).
- [55] A. O Caldeira and A. J Leggett, “Quantum tunnelling in a dissipative system,” *Ann. Phys.* **149**, 374–456 (1983).
- [56] M. Grifoni, M. Sasseti, and U. Weiss, “Exact master equations for driven dissipative tight-binding models,” *Phys. Rev. E* **53**, R2033–R2036 (1996).
- [57] M. Thorwart, M. Grifoni, and P. Hänggi, “Strong Coupling Theory for Tunneling and Vibrational Relaxation in Driven Bistable Systems,” *Ann. Phys.* **293**, 15–66 (2001).
- [58] L Magazzù, A. Carollo, D. Valenti, and B. Spagnolo, “Quantum dissipative dynamics of a bistable system in the sub-Ohmic to super-Ohmic regime,” *J. Stat. Mech.* **2016**, 054016 (2016).
- [59] M. Tsuchimoto and Y. Tanimura, “Spins Dynamics in a Dissipative Environment: Hierarchical Equations of Motion Approach Using a Graphics Processing Unit (GPU),” *J. Chem. Theory Comput.* **11**, 3859–3865 (2015).